Role of Nanostructured Dual-Oxide Supports in Enhanced Catalytic Activity: Theory of CO Oxidation Over Au/IrO$_2$/TiO$_2$

Zhi-Pan Liu, Stephen J. Jenkins, and David A. King*

Department of Chemistry, University of Cambridge, Lensfield Road, Cambridge CB2 1EW, United Kingdom
(Received 16 April 2004; published 6 October 2004)

The synergetic effect in multicomponent catalysts is a topic of profound industrial importance and intense academic interest. On a newly identified multicomponent catalyst, Au/IrO$_2$/TiO$_2$, first-principles density-functional theory is analyzed to clarify the outstanding catalytic activity of the system for oxidative reactions at high temperatures. By comparing CO oxidation on interfaces and single-component surfaces, it is revealed that a high dispersion of a more active oxide (IrO$_2$), on a more inert oxide (TiO$_2$) is the key. It preserves the sintering resistance of Au supported on less active oxides, while at the same time promoting oxidative reactions that occur at the Au/active-oxide interface.

Multicomponent catalysts, such as metal nanoparticles dispersed on oxide supports, often exhibit much higher activity than single-component catalysts. As a typical example of this synergetic effect, gold nanoparticles supported on certain oxides are revealed to be extremely active for low temperature oxidative reactions (e.g., below room temperature) [1,2]. It is found that not only the size of Au particles [2] but also the choice of oxide supports can be crucial for the performance of the Au/oxide catalysts [2–6]. To date, the physical origin of the catalytic role of oxide supports remains unclear, not least because of the complex nature of different supportive materials. In this Letter, we aim to provide insight into the support effects of Au-based catalysts, concentrating upon two key questions: (i) how does the support influence adsorption and sintering of the Au metal? and (ii) how does the support influence the reactivity in catalytic reactions?

Over the last ten years, CO oxidation on Au-based catalysts has been extensively studied. Intriguingly, it was found that Au supported on reducible oxides (e.g., TiO$_2$, Fe$_2$O$_3$, NiO$_x$) is at least 1 order of magnitude more active compared to Au supported on inert substrates (e.g., MgO, Al$_2$O$_3$, SiO$_2$) under similar conditions [3–6]. Focusing on the possible role of the oxide reducibility, Zhang *et al.* [7] found that a sputtered TiO$_2$ surface (with O vacancies) can limit cluster size and simultaneously increase the cluster density; more recently, Wahlstrom *et al.* [8] showed that oxygen vacancies on TiO$_2$ can serve as nucleation sites to immobilize Au particles. One major drawback of the Au/TiO$_2$ catalyst, however, is its low activity at the elevated temperatures (e.g., >450 K) required for many important industrial processes [2,9]. To overcome the problem, from recent experiments Okumura *et al.* [9] found that a Au/TiO$_2$ catalyst with added Ir shows much better catalytic activity for oxidative reactions at high temperatures (e.g., 473 K). Their transmission electron microscopy (TEM) analysis of a model Au-Ir-TiO$_2$ catalyst, [10] illustrated schematically in Fig. 1, showed that Ir is actually oxidized to IrO$_2$ during

the catalyst preparation [11], and that the three-component catalyst exhibits a surprisingly regular fungiform (i.e., mushroomlike) nanostructure: Au particles (5–10 nm) epitaxially cap IrO$_2$ pillars dispersed on TiO$_2$. These experimental studies demonstrated that the oxide support can radically alter the growth of metal particles and so the catalytic activity. To date, however, a general framework to understand the support effects is not established. Puzzling issues for which explanations remain elusive include the preferential bonding of Au on IrO$_2$ rather than TiO$_2$, and the high-temperature efficiency of the Au/IrO$_2$ interface for oxidative catalysis.

To understand these puzzles, we first compared Au adsorption on six different rutile-type oxides [13]: TiO$_2$, VO$_2$, CrO$_2$[13], RuO$_2$, IrO$_2$, and SiO$_2$. The first and last of the list are insulating, and the remainder are metallic. Trends in the Au-oxide bonding are crucial for our understanding of particle-support morphology, and the MO_2 (M: metal) rutile-type oxides were chosen as the model system because the rutile structure is one of the simplest and most common structural types adopted by many metal dioxides [13]. Amongst these, the rutile structure is the most stable form for $M =$ Ti, Ru, Ir, while for the others the rutile form is metastable, produced only under particular conditions [13]. The surface studied in each case is the low-index {110} face, which is generally the most stable facet for the rutile oxides. The {110} surface structure (Fig. 1 inset) exposes the bridging O atoms (the protruding rows) and the five-fold coordinated M (M_{5f}) ions. The oxide surfaces are modeled by 9-layer slabs with the top four layers relaxed and the others fixed at the bulk-truncated positions. All the calculations are performed using the total energy density-functional theory (DFT) approach with plane wave basis sets, as implemented in the CASTEP code [14]. The calculation details are described in Ref. [15].

By adding Au atoms onto the oxide surfaces (one Au atom per (1 × 2)-{110} unit cell), we have determined the binding energy of Au atoms on the stoichiometric surface,
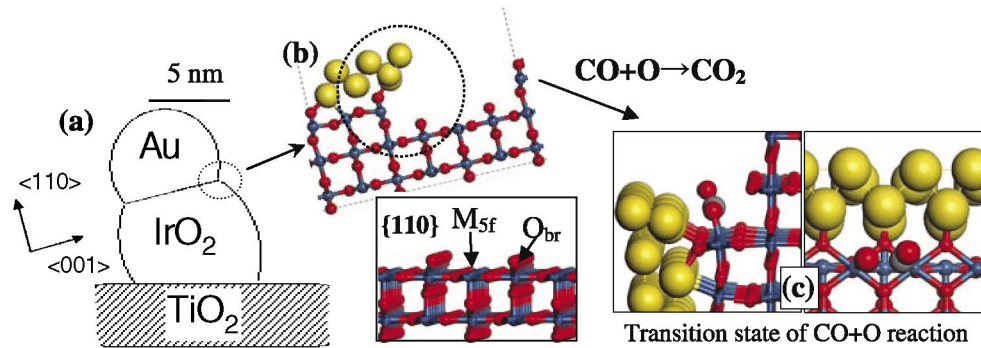
FIG. 1 (color online). (a) Experimentally observed fungiform nanostructure of the Au-IrO$_2$-TiO$_2$ catalyst [10]. (b) The modeling used in this work to describe the Au-IrO$_2$ interface. (c) The optimized structure (side and top view) of the transition state for CO oxidation at the Au/IrO$_2$ interface. For clarity, the {110} surface of rutile-type oxides is shown inset.

$E_{ad}^{Au/S}$, and on an O-vacant (reduced) surface, $E_{ad}^{Au/R}$. The results are listed in Table I. The O-vacant surface is modeled by removing half of the bridging O atoms from the stoichiometric surface (the formal oxidation state of the M ions adjacent to the O vacancy is thus reduced from +4 to +3). The energy (E_{O-vac}) required to create such an O-vacant surface is also calculated (see Table I) and constitutes an important measure of the reducibility of the oxide.

From Table I, we can see that E_{O-vac} follows the order: $SiO_2 > TiO_2 > RuO_2 > VO_2 > IrO_2 > CrO_2$. This is consistent with the general consensus that SiO_2 is an irreducible oxide, while it is rather easier to reduce the d-block metal oxides. As TiO_2 is commonly known as a reducible oxide, the d-block oxides studied here are all expected to be reducible under practical conditions. As for the Au adsorption energy, we found that in the d-block oxides, $E_{ad}^{Au/S}$ increases monotonically with d-band occupation, while in the p-block oxide SiO_2 its value is small and similar to that of the early d-block oxides TiO_2 and VO_2. Furthermore, $E_{ad}^{Au/R}$ is generally substantially larger than $E_{ad}^{Au/S}$, except for CrO_2 where the two are similar. These results indicate that the nucleation of Au will typically occur at O-vacancy sites except for strongly reducible oxides, such as CrO_2. More importantly, we identified that the bonding of Au with IrO_2 is

intrinsically strong compared to other oxides. This supports the experimental finding [10] that Au will preferentially grow on IrO_2 in a TiO_2-IrO_2 binary system.

To understand the origin of this Au/IrO$_2$ bonding, we calculated the electron density change upon Au adsorption on stoichiometric IrO$_2${110}, which is further compared with that for Au on stoichiometric TiO$_2${110}, as shown in the contour plots of Fig. 2(a) and 2(b) (see Fig. 2 caption for details). From these figures, we can see that the Au/IrO$_2$ bonding is basically quite similar to the Au/TiO$_2$ bonding except that the electron density variation is more pronounced in the Au/IrO$_2$ system. Fundamentally, these bonding features can be understood as follows. TiO$_2$ is an insulator with a band gap of more than 2 eV. In TiO$_2${110}, the d states of Ti$_{5f}$ are largely unoccupied, as illustrated in Fig. 2(c), which shows the density of states projected onto the d orbitals of a Ti$_{5f}$ atom on clean TiO$_2${110}. The bonding of Au with Ti therefore does not involve a significant contribution from the d electrons of Ti. In contrast, IrO$_2$ is metallic,

TABLE I. Maximum Au adatom bonding energy on the {110} surface of six different rutile-type (MO_2) oxides, including the stoichiometric ($E_{ad}^{Au/S}$) and the O-vacant ($E_{ad}^{Au/R}$) surfaces [15]. The formal valence electronic configuration of the M^{4+} ion, and the energy to create the O-vacant surfaces (E_{O-vac}) are also listed.

	TiO$_2$	VO$_2$	CrO$_2$	RuO$_2$	IrO$_2$	SiO$_2$
M^{4+}	d^0	d^1	d^2	d^4	d^5	p-block
E_{O-vac}	6.35	5.00	3.41	5.24	4.83	8.32
$E_{ad}^{Au/S}$	0.87	0.99	1.56	1.68	2.27	0.94
$E_{ad}^{Au/R}$	2.87	1.96	1.51	2.90	3.37	2.25

FIG. 2 (color online). Contour plots of electron density difference cutting through (a): a Au-Ir$_{5f}$ bonding plane in the Au/IrO$_2$ system and (b): a Au-Ti$_{5f}$ bonding plane in the Au/TiO$_2$ system. The positive/negative values ($e/$ Å^3) are electron density increase or decrease upon Au adsorption. Also shown are plots of the density of states projected onto (c): the d orbitals of the Ir$_{5f}$ atom at a clean IrO$_2${110} surface and (d): the Ti$_{5f}$ atom at a clean TiO$_2${110} surface. The Fermi level is set to be the energy zero.

with its Fermi level crossing the d states of the Ir ions. The Fermi level states of the Ir_{5f} atom in $IrO_2\{110\}$ exhibit mainly t_{2g} (d_{xy}, d_{yz}, and d_{xz}) symmetry and are either nonbonding or antibonding in character. This is illustrated in Fig. 2(d), which shows the density of states projected onto the d orbitals of an Ir_{5f} atom on clean $IrO_2\{110\}$. Upon adsorption of the Au atom, the unoccupied d_{z^2} state of the Ir atom can form a covalent bond with the Au $6s$ orbital leading to a new bonding state d_{z^2}(Ir)-s(Au) lying below the Fermi level. Consequently, the t_{2g} electrons at the Fermi level of the Ir atom will flow into this new state, accounting both for the enhanced bonding of Au on IrO_2 and for the pattern of electron density redistribution observed. This bonding picture also explains the magnetic property of the adsorbed Au atom, which remains spin-polarized in the Au/TiO_2 system, but becomes non spin-polarized in the Au/IrO_2 system.

According to the data in Table I, we can further predict the sintering tendency of Au particles on the oxides. For the reducible oxides, the Au particles will typically nucleate at the O-defect sites. Heating the system, however, will inevitably lead to the sintering of Au particles because the Au metal cohesive energy (calculated as $E_{coh}^{Au} = 3.2$ eV) is generally larger than the Au-oxide bonding energy (Table I). Since sintering occurs via migration of Au monomers across the unreduced oxide surface, the growth kinetics of Au particles will be controlled by the term $\exp[(-\Delta E/RT)]$, where ΔE is the barrier for a Au monomer moving from a small particle to a larger particle [19,20]. For a support comprising a single oxide species, therefore, ΔE should be close to E_{coh}^{Au} minus $E_{ad}^{Au/S}$ [19,20]. To compare different oxides, it can be deduced that a large $E_{ad}^{Au/S}$ corresponds to a fast sintering speed. As the d-band occupation increases, therefore, the sintering speed of Au particles on the d-block oxides will become faster, leading to the formation of larger Au particles. Such an analysis therefore suggests that sintering would be least problematic on TiO_2 but most troublesome on IrO_2. When the support features two different oxides, however, Au will cluster on the material for which $E_{ad}^{Au/R}$ is largest (IrO_2 in our

case), and its migration to an adjacent particle is hindered by the large energy barrier in crossing to the other oxide (TiO_2 in our case). Thus, the Au particle distribution is largely dictated by that of the IrO_2 pillars and sintering is strongly suppressed. The key to an active catalyst of long-term stability is thus the manufacture of a suitably-dispersed dual-oxide support matrix.

Having thus dealt with sintering issues, it is now essential to understand why IrO_2 can boost the catalytic ability of the Au/TiO_2 catalyst at high temperatures. Using CO oxidation as the model reaction, we studied possible mechanisms at the Au/IrO_2 interface. According to the TEM analysis [10], Au particles grow epitaxially on IrO_2 with the Au{100} plane lined up against the $IrO_2\{110\}$ face [15]. The Au/IrO_2 interface (the circled region in Fig. 1(a)] is at the edge of the $IrO_2\{110\}$ plane in contact with the perimeter of the Au particles. In our calculation, this interface is modeled by a two-layer Au strip on the top of a stepped $IrO_2\{110\}$ surface (circled region in Fig. 1(b)] [15].

Molecular O_2 and CO adsorption energies are calculated and listed in Table II. Without Au particles, the O_2 molecule is found to adsorb strongly on clean stoichiometric $IrO_2\{110\}$ with an adsorption energy of 1.11 eV per molecule. The dissociation of O_2 on this surface is, however, endothermic by 0.95 eV per molecule. In the presence of Au, the O_2 adsorption energy at the Au/IrO_2 interface increases up to 1.42 eV, and more importantly, the dissociation of O_2 now becomes facile. The barrier to O_2 dissociation is only 0.22 eV and the whole process is exothermic by 0.30 eV per molecule. We found that this is due to a pronounced increase in O atom adsorption energy at the Au/IrO_2 interface (3.48 eV) compared to the $IrO_2\{110\}$ surface (2.70 eV). This additional bonding energy arises from the newly-developed O-Au interaction at the interface. For CO adsorption, in contrast, we found that the molecule can already adsorb strongly on clean stoichiometric $IrO_2\{110\}$ with adsorption energy 2.18 eV, and this value remains similar when it coadsorbs with O at the interface. As O_2 dissociation can occur readily, CO oxidation at the Au/IrO_2 interface presumably follows by a monomolecular $CO + O \rightarrow CO_2$ mechanism, as opposed to the mechanism deduced previously for CO oxidation on Au/TiO_2, where a bimolecular pathway, $CO + O_2 \rightarrow CO_2 + O$, was preferred [16,18,21]. By bringing CO and O together at the interface of Au/IrO_2 through constrained minimisation, we have located a pathway leading to CO_2 formation. The top and side views of the transition state are shown in Fig. 1(c). The barrier to the monomolecular CO reaction is found to be 0.62 eV, which is similar to that of the same reaction on pure $IrO_2\{110\}$ reported previously [17] where the low barrier of CO oxidation on oxide has been attributed to the high reactivity of the adsorbed O atom. The crucial role of the Au/IrO_2 interface is primarily to provide the active O atoms necessary for this favorable reaction to occur.

TABLE II. Comparison of CO oxidation on Au/TiO_2 (from Ref. [16]) and Au/IrO_2 systems. The unit of energy is eV.

	$E_{ad}(O_2)$	$E_{ad}(CO)$	$E_a^{(O_2\rightarrow 2O)}$	$E_a^{(CO\ oxidation)}$
Au/TiO_2	0.60[a]	1.38[b]	0.52	0.17[d]
Au/IrO_2	1.42[a]	2.10[a,c]	0.22	0.62[e]
IrO_2	1.11	2.18	$\cdots$	0.61[f]

[a] Adsorbed at interface-adjacent oxide;
[b] Adsorbed on Au (step edge);
[c] In presence of preadsorbed O;
[d] $CO + O_2 \rightarrow CO_2 + O$;
[e] $CO + O \rightarrow CO_2$;
[f] Ref. [17].

Comparing CO oxidation on Au/IrO_2 with that on Au/TiO_2, which was calculated previously, [16] we can see two major differences between the two systems: (i) IrO_2 can bond reactants CO and O_2 much more strongly than can TiO_2, which is essential for the reaction to occur at high temperatures, and (ii) the catalytic role of Au in Au/IrO_2 is mainly to promote O_2 dissociation to provide active atomic O, while in the Au/TiO_2 system, Au particles provide the bonding site for CO and are directly involved in CO oxidation [16,21]. Our calculations not only explain the enhanced catalytic ability of the Au/IrO_2 system at high temperatures, but also demonstrate that the mechanism of CO oxidation can be fundamentally dependent upon the choice of support material.

In summary, the present DFT calculations on the $Au/IrO_2/TiO_2$ system provide a convincing first-principles theoretical framework within which the synergetic effect in complex multioxide catalysts may be understood. First, we have demonstrated and explained the preferential Au adsorption on late transition metal oxides and the anti-sintering property of Au on early transition metal oxides. Second, we have shown that the introduction of the dual-oxide support permits the presence of an active Au/IrO_2 interface while preserving the excellent resistance against sintering characteristic of the Au/TiO_2 system. Our new mechanism involves strongly-bound reactants and dissociated O atoms on the Au/IrO_2 interface, and convincingly explains the high-temperature activity of the system. Whilst the details of this framework will doubtless differ from case to case, we nevertheless expect the underlying logic outlined here to be transferable to studies of a variety of multioxide supported catalytic systems.

---

*Author to whom correspondence should be addressed.
Electronic address: dak10@cam.ac.uk

[1] M. Haruta, Catal Today **36**, 153 (1997).

[2] M. Valden, X. Lai., and D. W. Goodman, Science, **281**, 1647 (1998).

[3] J. D. Grunwaldt, C. Kiener, C. Wogerbauer, and A. Baiker, J. Catal. **186**, 458 (1999).

[4] F. Cosandey and T. E. Madey, Surf. Rev. Lett. **8**, 73 (2001).

[5] M. Schubert *et al.*, J. Catal. **197**, 113 (2001).

[6] L. Guczi *et al.*, J. Am. Chem. Soc. **125**, 4332 (2003).

[7] L. Zhang *et al.*, Surf. Sci. **439**, 73 (1999).

[8] E. Wahlstrom *et al.*, Phys. Rev. Lett., **90**, 026101 (2003).

[9] M. Okumura *et al.*, Appl. Catal., B **41**, 43 (2003).

[10] T. Akita *et al.*, J. Electron Microsc. **52**, 119 (2003).

[11] Ir oxidation can occur in air at 573–773 K (T. Wang and L. D. Schmidt, J. Catal. **66**, 301 (1980)). Our DFT calculation also confirmed this (see Ref. [12(b)]).

[12] (a) Z.-P. Liu, S. J. Jenkins, and D. A. King, J. Am. Chem. Soc., **125**, 14660 (2003).(b) Z.-P. Liu, S. J. Jenkins, and D. A. King, J. Am. Chem. Soc. **126**, 10 746 (2004).

[13] See, e.g., A. A. Bolzan *et al.*, Acta Crystallogr. Sect. B **53**, 373 (1997) and the references therein.

[14] M. C. Payne *et al.*, Rev. Mod. Phys. **64**, 1045 (1992).

[15] For the data shown in Table I, a (1×2-{110}) unit cell is always used and Au adatoms adsorb on one side of the slab. Convergence has been examined by allowing the Au adsorbate to adsorb on both sides of slab, and the energy difference is found to be always within 0.1 eV. On the stoichiometric {110} surfaces, the most stable site for the Au adatom adsorption is always close to the top site of the M_{5f} ion, and on the reduced surfaces it is at the O-vacancy site. For the data shown in Table II, a (3×2)-{110} unit cell (in all 36 units of IrO_2 per stoichiometric slab) is used, which is large enough to accommodate a Au/IrO_2 interface (Fig. 1). The $Au/IrO_2/TiO_2$ structure observed experimentally [10] has been checked by our calculation, which confirmed that (i) IrO_2 tends to cluster on TiO_2, as the binding energy of an IrO_2 overlayer on IrO_2{110} is much larger than that of an IrO_2 overlayer on TiO_2{110}; and (ii) the Au{100}/IrO_2{110} growth is energetically more favored compared to a Au{111}/IrO_2{110} growth. The sides of the modeled Au strip [Fig. 1(b)] are {111} facets to minimize the surface energy. The other parameters in the CASTEP calculation are the same as described in Refs. [12,16–18].

[16] Z.-P. Liu *et al.*, Phys. Rev. Lett. **91**, 266102 (2003).

[17] X.-Q. Gong, Z.-P. Liu, R. Raval, and P. Hu, J. Am. Chem. Soc. **126**, 8 (2004).

[18] Z.-P. Liu, P. Hu, and A. Alavi, J. Am. Chem. Soc., **124**, 7499 (2002).

[19] C. T. Campbell, S. C. Parker, and D. E. Starr, Science, **298**, 811 (2002).

[20] We have calculated the diffusion of a single Au atom along the trough of IrO_2{110} and on TiO_2{110}. In both cases, diffusion is found to be facile, with the barrier less than 0.5 eV. The overall barrier to diffusion is therefore totally determined by the barrier of Au moving from the Au particle onto the oxide, and from one oxide to the other.

[21] L. M. Molina and B. Hammer, Phys. Rev. Lett. **90**, 206102 (2003); L. M. Molina, M. D. Rasmussen, and B. Hammer, J. Chem. Phys. **120**, 7673 (2004).